1 **Title:**

2 Celecoxib does not protect against fibrosis and inflammation in a carbon tetrachloride-induced

3 model of liver injury

4

5 **Authors:**

6 Todd R. Harris, Sean Kodani, Amy A. Rand, Jun Yang, Denise M. Imai, Sung Hee Hwang, and

7 Bruce D. Hammock

8 Laboratory of origin: B.D.H.

9 Department of Entomology and Nematology and UC Davis Comprehensive Cancer Center,

10 University of California, Davis, 1 Shields Avenue, Davis, California, USA, 95616 (T.R.H., S.K.,

11 A.R., J.Y., S.H.H., B.D.H.).

12 Comparative Pathology Laboratory, School of Veterinary Medicine, University of California,

13 Davis, 1 Shields Avenue, Davis, California, USA 95616 (D.M.I.).

14

15

16

17

18

19

20

21

22

23

1 **Running Title: Celecoxib Modulates Carbon Tetrachloride Fibrosis**

2 Corresponding Author: Bruce D. Hammock, Department of Entomology and Nematology and UC

3 Davis Comprehensive Cancer Center, University of California, Davis, 1 Shields Avenue, Davis,

4 California, USA, 95616. Tel: (530) 752 7519; Fax: (530) 752-1537; E-mail:

5 bdhammock@ucdavis.edu.

6 Number of text pages: 32

7 Number of tables: 1

8 Number of references: 33

9 Number of words in Abstract: 240

10 in Introduction: 552

11 in Discussion: 1500

12 Abbreviations:

13 APAP: Acetaminophen; BDL: Bile duct ligation; CCl_4: Carbon Tetrachloride; COL1A1: Collagen

14 1A1; COX: Cyclooxygenase; CUDA: 12-(3-cyclohexyl-ureido)dodecanoic acid; CYP:

15 Cytochrome P450; DHET: Dihydroxyeicosatrienoic acids; EET: Epoxyeicosatrienoic acid; EpFA:

16 Epoxy fatty acids; ER: Endoplasmic reticulum; HSC: Hepatic stellate cell; LOX: Lipoxygenase;

17 LXA_4: Lipoxin A4; MMP: Matrix metalloprotease; NSAID: Non-steroidal anti-inflammatory

18 drug; PGD_2: Prostaglandin D2; PGE_2: Prostaglandin E2; PGI_2: Prostaglandin I2; PGJ_2:

19 Prostaglandin J2; PTUPB: 4-(5-phenyl-3-{3-[3-(4-trifluoromethylphenyl)-ureido]-propyl}-

20 pyrazol-1-yl)-benzenesulfonamide; sEH: Soluble epoxide hydrolase; sEHI: Soluble epoxide

21 hydrolase inhibitor; SMA: Smooth muscle actin; TAA: Thioacetamide; TIMP: Tissue inhibitors

22 of metalloproteases; TGF: Transforming growth factor; TPPU: 1-trifluoromethoxyphenyl-3-(1-

23 propionylpiperidin-4-yl) urea; TXA_2:Thromboxane A2.

1 **Abstract**

2 The cyclooxygenase-2 (COX-2) selective inhibitor, celecoxib, is widely used in the treatment of

3 pain and inflammation. Recently, celecoxib has been explored as a possible treatment for liver

4 fibrosis with contradictory results depending on the model. The present study reports the effect of

5 celecoxib in a five week carbon tetrachloride (CCl_4)-induced liver fibrosis mouse model.

6 Celecoxib alone and a combination of celecoxib and inhibitors of the enzyme soluble epoxide

7 hydrolase (sEH) as well as a dual inhibitor that targets both COX-2 and sEH were administered

8 via osmotic minipump to mice receiving intraperitoneal injections of CCl_4. We found that there

9 was elevated collagen deposition in the mice treated with both celecoxib and CCl_4 compared to

10 the Control or CCl_4 only groups, as assessed by trichrome staining. Histopathology revealed more

11 extensive fibrosis and cell death in the animals treated with both celecoxib and CCl_4 compared to

12 all other experimental groups. While some markers of fibrosis, such as MMP-9, were unchanged

13 or lowered in the animals treated with both celecoxib and CCl_4, overall, the hepatic fibrosis was

14 more severe in this group. Co-treatment with celecoxib and an inhibitor of sEH or treatment with

15 a dual inhibitor of COX-2 and sEH decreased the elevated levels of fibrotic markers observed in

16 the group that received both celecoxib and CCl_4. Oxylipid analysis revealed that celecoxib reduced

17 the level of PGE_2 relative to the CCl_4 only group. Overall, celecoxib treatment did not decrease

18 liver fibrosis in CCl_4 treated mice.

19

20

21

22

23

MOL #111831

1   **Introduction**

2   Celecoxib is a non-steroidal anti-inflammatory drug used by millions of patients to

3   alleviate the pain and inflammation associated with diseases such as rheumatoid arthritis (Bessone

4   et al., 2016). Reviews of controlled trials have found no significant difference in the incidence of

5   liver damage between patients administered celecoxib and those receiving placebo (Bessone et al.,

6   2016).

7   Liver fibrosis is the result of a normally beneficial wound healing process that can be

8   initiated by toxicants such as ethanol or carbon tetrachloride (Liedtke et al., 2013). This

9   inflammatory process involves the activation of resident macrophages called hepatic stellate cells

10   (HSCs) and the recruitment of macrophages, both of which express pro-inflammatory signaling

11   molecules, along with enzymes and structural proteins that remodel the extra-cellular matrix

12   (Pellicoro et al., 2014). This remodeling includes the increased deposition of matrix proteins such

13   as collagen, as well as changes in the populations of metalloproteases (Pellicoro et al., 2014). If

14   damage due to exposure to the toxicant continues, liver fibrosis will alter the architecture of the

15   organ and lead to liver failure (Liedtke et al., 2013).

16   Due to its anti-inflammatory effect, celecoxib has been explored as a possible therapy in

17   several models of liver fibrosis, such as the thioacetamide (TAA)- and carbon tetrachloride (CCl_4)-

18   induced rodent models and the surgical bile duct ligation (BDL) rodent model. CCl_4 acts primarily

19   through an increase in hepatic lipid peroxidation and oxidative stress while TAA acts primarily

20   through an increase in oxidative stress, processes which damage hepatocytes and trigger fibrosis

21   (Martinez et al., 2014). BDL is a surgical model in which the bile duct is partially ligated, leading

22   to cholestasis, liver damage and fibrosis (Martinez et al., 2014). In some models, treatment with

23   celecoxib has resulted in a reduction in fibrosis and inflammation, while in others, including some

4

1   rat CCl_4-induced models, celecoxib has worsened the liver damage and fibrosis (Chavez et al.,

2   2010; Hui et al., 2006; Paik et al., 2009).

3   Celecoxib targets cyclooxygenase 2 (COX-2), an enzyme that metabolizes arachidonic acid

4   to a class of oxidized fatty acids called prostaglandins (Shi and Klotz, 2008). These oxylipids have

5   diverse effects in the liver, but many COX-2 metabolites increase inflammation and portal

6   hypertension (Sacerdoti et al., 2015). Arachidonic acid is also metabolized by cytochrome P450s

7   to form the epoxyeicosatrienoic acids (EETs) (Morisseau and Hammock, 2013). The EETs have

8   been investigated in several disease models and have been found to be anti-inflammatory, organ

9   protective, and anti-fibrotic in heart and kidney models of fibrosis (Morisseau and Hammock,

10   2013). The EETs are further metabolized by soluble epoxide hydrolase (sEH) to the

11   dihydroxyeicosatrienoic acids (DHETs) that are less lipophilic and more readily conjugated and

12   excreted by the organism (Morisseau and Hammock, 2013).

13   We previously modulated the oxylipids in a CCl_4-induced model of hepatic fibrosis

14   through the use of dietary manipulation of lipid intake as well as inhibition of sEH, which blocks

15   the major route of metabolism of the EETs and other epoxy fatty acids (Harris et al., 2015; Harris

16   et al., 2016). In general, perturbation of the oxylipids with sEH inhibitors reduced collagen

17   deposition in addition to the expression and activity of pro-fibrotic MMPs (Harris et al., 2015;

18   Harris et al., 2016). These results raised the question of how celecoxib, another modulator of

19   oxylipids, would impact fibrosis in the CCl_4 model and whether tools we developed for inhibiting

20   both sEH and COX-2 would alter the observed effects of COX-2 inhibition.

21   In this study, we treated mice with CCl_4 over a five-week period to induce liver fibrosis.

22   Interestingly, we found that markers of fibrosis were elevated in the mice that received both

23   celecoxib and CCl_4 compared to those animals receiving CCl_4 alone. Modulation of the EETs by

1   either an sEH inhibitor or a dual inhibitor of COX-2 and sEH, blunted some aspects of the pro-

2   fibrotic effect of COX-2 inhibition in the CCl_4 background.

3

4

5

6

7

8

9

10

11

12

13

14

15

16

17

18

19

20

21

22

23

1   **Materials and Methods**

2   Animals

3   Male C57BL/6NCrl mice (~25g) were obtained from Charles River, Inc. (Wilmington, MA, USA)

4   one week prior to the experiment and kept on a 12h/12h light/dark cycle. The animal protocol was

5   approved by University of California Davis Institutional Animal Care and Use Committee and the

6   study was performed in accordance with the National Institutes of Health guide for the care and

7   use of laboratory animals.

8

9   Chemicals

10 All commercial chemicals were purchased from Sigma (St. Louis, MO, USA) unless otherwise

11 noted. TPPU, 1-(4-trifluoromethoxyphenyl)-3-(1-propionylpiperidin-4-yl)-urea, and PTUPB, 4-

12 (5-phenyl-3-{3-[3-(4-trifluoromethylphenyl)-ureido]-propyl}-pyrazol-1-yl)-benzenesulfonamide,

13 were synthesized according to the previous procedures (Hwang et al., 2011; Rose et al., 2010).

14 Celecoxib was a gift from Pfizer (New York, NY, USA). Structures of TPPU, PTUPB and

15 Celecoxib are given in Supplemental Data Figure S1.

16

17 Experimental Design

18 The mice were randomly divided into five experimental groups (6 animals/group): (1) Control,

19 (2) CCl_4 only, (3) Celecoxib+CCl_4, (4) Celecoxib+TPPU+CCl_4, (5) PTUPB+CCl_4. CCl_4 was

20 administered following a protocol described in detail in (Constandinou et al., 2005). Briefly, CCl_4

21 was mixed 1:1 (v/v) with Neobee M5 (Sigma, St. Louis MO, USA) and injected i.p. every five

22 days for a total of seven injections of 80 mg/kg. Mice were euthanized three days after the final

23 injection. Celecoxib, PTUPB, and a combination of celecoxib and TPPU were administered

1   subcutaneously via Alzet model 2006 osmotic minipumps (Cupertino, CA, USA). These pumps

2   produce a 3.6 µL/day continuous flow rate for up to 45 days. The Control group received Neobee

3   M5 only. The Control group and CCl_4 only group were implanted with minipumps filled with the

4   1:1 (v/v) PEG400:DMSO solution.

5

6   Plasma blood level analysis

7   Mouse plasma (10 µL) was mixed with 50 µL of water containing 0.1% formic acid. The liquid-

8   liquid extraction and LC-MS/MS analysis were previously performed as described (Harris et al.,

9   2016).

10

11   Determination of liver tissue hydroxyproline levels

12   Hydroxyproline content was determined following a method in (Reddy and Enwemeka, 1996).

13   Briefly, 10 µL of 10 N NaOH was added to 40 µL of 0.33 mg/µL liver tissue homogenate and the

14   solution was autoclaved at 120 °C for 25 min. After the reaction cooled to room temperature,

15   chloramine T reagent (0.84% chloramine-T, 42 mM sodium acetate, 2.6 mM citric acid, and 39.5%

16   isopropanol) was added (450 µL) bringing the volume to 500 µL. After incubation at room

17   temperature for 25 min, DMAB reagent, 15% 4-(dimethylamino)benzaldehyde in 2:1 (v/v)

18   isopropanol/perchloric acid mixture, was added (500 µL) bringing the volume to 1 mL. The

19   solution was then incubated at 65 °C for 20 min and the absorbances of the samples measured at

20   550 nm.

21

22   mRNA transcript analysis

1   Liver tissue was immediately stored in RNA later solution (Thermo Fisher Scientific, Waltham,

2   MA USA) for 24 h at 4 °C before freezing at -80 °C. Tissue was homogenized using a roto stator

3   grinder (IKA Works Inc., Wilmington, NC, USA) and passed through a QIAshredder column

4   (Qiagen, Valencia, CA, USA). Total RNA was purified using RNeasy kit (Qiagen). cDNA

5   synthesis from total RNA was performed by the QuantiTect Reverse Transcription Kit (Qiagen).

6   RTPCR was performed using an Applied Biosciences Fast 7500 Real-Time PCR System (Foster

7   City, CA, USA). The following Taqman probes were purchased from Life Technologies

8   Corporation: GAPDH, Mm99999915_g1; TGFB1, Mm01178820_m1; MMP-2,

9   Mm00439498_m1; MMP-9, Mm00442991_m1; COL1A1, Mm00801666_g1; TIMP-1,

10   Mm00441818_m1 (Life Technologies Corp., Grand Island, NY, USA). GAPDH was used as the

11   internal control.

12

13   Histopathology scoring

14   Liver samples were immersion-fixed in 10% neutral-buffered formalin for 48 hours. Samples were

15   stored in 70% (v/v) ethanol in distilled deionized water prior to routine processing. Tissues were

16   processed, embedded in paraffin, sectioned and stained with hematoxylin and eosin (H&E) by the

17   Histopathology service in the UC Davis Veterinary Medical Teaching Hospital (Davis, CA, USA).

18   H&E-stained sections of liver were scored for inflammation, fibrosis and cellular damage by a

19   board-certified laboratory animal pathologist (DMI). The scoring system is reported in

20   Supplemental Data Table S1.

21

22   Trichrome staining and Immunohistochemistry

23   αSMA and F4/80 immunohistochemistry and trichrome staining were performed by the Genomic

9

1   Pathology Laboratory at UC Davis and quantitated using imaging analysis software from Aperio

2   (Sausalito, CA, USA) using the IHC and positive pixel count (PPC) algorithms.

3

4   <u>Oxylipid analysis</u>

5   Oxylipids in the COX and LOX branches of the arachidonic acid cascade were extracted and

6   detected as described (Harris et al., 2016). Oxylipids in the P450 branch of the arachidonic acid

7   cascade were detected as follows. Samples were analyzed on a Waters Acquity Ultra

8   Performance Liquid Chromatograph coupled to a Waters Xevo TQ-S Mass Spectrometer in

9   negative electrospray ionization mode. Samples were injected (5 µL) and separated using a

10   Phenomenex Kinetex column (150 x 2.1 mm; 1.7 µm) at 40°C using the following mobile phase

11   gradient, consisting of water (A) and acetonitrile (B) each containing 0.1% acetic acid: initial

12   conditions of 65:35 A:B for 2.9 min ($t = 2.9$ min), changing to 45:55 at 3 min ($t = 3$ min) and

13   decreasing to 35:65 over 5.5 min ($t = 8.5$), decreasing to 5:95 over 4 min ($t = 12.5$), holding at

14   5:95 for 1 min ($t = 13.5$), reverting to initial conditions of 65:35 in 0.1 min ($t = 13.6$ min) and re-

15   equilibrating for 1.9 min ($t = 15.5$ min). Mass spectral analysis was accomplished using a

16   capillary voltage of 3 kV, a desolvation temperature of 200°C, a desolvation gas flow of 800

17   L/hr, a cone gas flow of 150 L/hr, nebulizer pressure of 6 bar, and collision gas flow of 0.15

18   mL/min. Mass transitions for each EET were as follows: 14,15-EET (319.0 > 219.0); 11,12-EET

19   (319.0 > 167.0); 8,9-EET (319.0 > 155.0). Analyte concentration was quantified against an

20   internal standard calibration curve, normalizing analyte response to 11,12-EET-d_{11} (330.2 >

21   167.2), and 12-(3-cyclohexyl-ureido)dodecanoic acid (CUDA, 341.3 > 216.4) to correct

22   extraction efficiency and instrument response, respectively. Dwell time for each analyte was 25

23   ms. The detailed information for all analytes are reported in Supplemental Data Table S2.

MOL #111831

1

2   Statistics

3   Normality was assessed by the Shapiro-Wilk test. Significance was determined by one-way

4   ANOVA followed by the Dunnett multiple comparison test. All statistical calculations were

5   performed using SigmaPlot (Systat Software, Inc., San Jose, CA, USA).

6

7

8

9

10

11

12

13

14

15

16

17

18

19

20

21

22

23

11

MOL #111831

1   **Results**

2   **Subcutaneous osmotic minipumps produced high plasma concentrations of celecoxib**

3   Male C57BL mice were implanted with osmotic minipumps two days before the start of

4   CCl_4 exposure via i.p. injections as described in Materials and Methods. The five experimental

5   groups were (1) Control, (2) CCl_4 only, (3) Celecoxib+CCl_4, (4) Celecoxib+TPPU+CCl_4, and (5)

6   PTUPB+CCl_4. The drugs were loaded into minipumps so that the calculated dose of each

7   compound would be 10 mg/kg/day.

8   When we examined plasma levels of the drugs, we found that the TPPU and celecoxib

9   levels in the Celecoxib+TPPU+CCl_4 group were 1.11±0.018 µM and 1.32±0.039 µM,

10   respectively. The plasma concentration of celecoxib in the Celecoxib+CCl_4 group was 1.58±0.47

11   µM and the PTUPB concentration in the PTUPB+CCl_4 group was 0.65±0.027 µM. These plasma

12   concentrations are far above the IC_{50} of for celecoxib and TPPU with their respective target mouse

13   enzymes and approximately half the IC_{50} for PTUPB with human COX-2 and far above the IC_{50}

14   for PTUPB with human sEH. Despite developing robust fibrosis after the five week CCl_4

15   treatment, the weight of the mice increased, with no statistical difference between the groups (*p-*

16   *value* < 0.05), the CCl_4 toxicity being less severe than other models (Supplemental Data Figure

17   S2).

18   **Celecoxib increased collagen deposition and liver damage in CCl_4 treated mice**

19   Trichrome staining revealed that the Celecoxib+CCl_4 had a higher amount of collagen

20   deposition than the CCl_4 only group (Figure 1, A-F). The PTUPB+CCl_4 group had a reduced level

21   of collagen deposition when compared to the Celecoxib+CCl_4 group, though still higher than the

22   Control group (Figure 1F). Hydroxyproline levels in hepatic tissue from the Celecoxib+CCl_4 group

23   was the same as CCl_4 only group (*p*-value > 0.05), and the levels from both the

12

1   Celecoxib+TPPU+CCl4 and PTUPB+CCl4 groups were lower than the CCl4 only group (Figure

2   1G).

3   We next performed a histopathological assessment of the extent of liver fibrosis and

4   damage (Table 1). The categories were defined as follows: vacuolation: lacy or vacuolated

5   cytoplasm that distends the hepatocyte; necrosis: single cell death of hepatocytes in centrilobular

6   to random areas; lipofuscinosis: accumulation of lipid pigments, associated with nondegradable

7   cellular breakdown products in macrophages; fibrosis: fibroblast proliferation with increased

8   deposition of collagen around centrilobular regions occasionally connecting between centrilobular

9   regions (bridges) or extending into the surrounding parenchyma (dissecting); inflammation: mixed

10   neutrophilic and mononuclear inflammation around predominantly centrilobular regions. The

11   slides were read in a blind fashion. The scoring system is reported in Supplemental Data Table S1.

12   The Celecoxib+CCl4 group had the highest composite lesion scores due to greater indices of

13   hepatocellular damage (vacuolar degeneration, necrosis, fibrosis, regeneration). When the

14   Celecoxib+TPPU+CCl4 group was examined, it was found that the addition of TPPU dampened

15   the effect of celecoxib (p-value = 0.0117), predominantly by decreasing hepatic necrosis (p-value

16   = 0.0256) and regeneration (p-value = 0.0134).

17   **Celecoxib did not significantly raise the level of pro-fibrotic markers in CCl4 treated mice**

18   To further gauge the extent of fibrosis, we measured the mRNA level of common markers

19   by RTPCR (Figure 2). The expression levels of collagen 1A1 (COL 1A1) was increased in the

20   CCl4 only group compared to the Control group (p-value < 0.05), and further increased in the

21   Celecoxib+CCl4 group, but this difference did not reach statistical significance (p-value > 0.05)

22   (Figure 2A). The mRNA expression of MMP-2 and MMP-9 were also elevated in the CCl4 only

23   group (Figure 2B and C). For MMP-2, the three treatment groups were no different than the CCl4

1   only group (Figure 2B). In the case of MMP-9, levels in the Celecoxib+CCl$_4$,

2   Celecoxib+TPPU+CCl$_4$ and PTUPB+CCl$_4$ groups, while not different than CCl$_4$ only group, were

3   also not different than the Control group (p-value > 0.05) (Figure 2C). TIMP-1 was elevated in the

4   CCl$_4$ only group, but the further increase observed in the Celecoxib+CCl$_4$, Celecoxib+TPPU+CCl$_4$

5   and PTUPB+CCl$_4$ groups did not reach significance (Figure 2D). For TGF-β, the levels of the

6   Celecoxib+CCl$_4$ and Celecoxib+TPPU+CCl$_4$ groups were lower than the CCl$_4$ only group, but this

7   difference did not reach statistical significance (Figure 2E).

8   **Celecoxib increased αSMA but not F4/80 staining in CCl$_4$ treated mice**

9   F4/80 is a mouse cell surface protein expressed in many populations of macrophages. CCl$_4$

10   increased the F4/80 immunohistochemical staining relative to the Control group (Figure 3). While

11   the amount of positive staining in the Celecoxib+CCl$_4$, PTUPB+CCl$_4$, and Celecoxib+TPPU+CCl$_4$

12   groups were not significantly reduced (p-value > 0.05) when compared with the CCl$_4$ only group

13   (Figure 3F), these groups were also not different than the Control group.

14   To assess hepatic stellate cell (HSC) activation, we performed IHC on liver tissue with an

15   anti-αSMA (smooth muscle actin) antibody (Figure 4). We found that HSC activation was greatest

16   in the Celecoxib+CCl$_4$ group, where it was significantly increased relative to both the Control and

17   CCl$_4$ only groups (p-value < 0.05). Co-treatment with celecoxib and TPPU or treatment with

18   PTUPB in the CCl$_4$ background decreased the level of HSC activation compared to the animals

19   receiving celecoxib and CCl$_4$. In the case of the Celecoxib+TPPU+CCl$_4$ group, the HSC activation

20   was significantly less than the Celecoxib+CCl$_4$ group (p-value < 0.05). In the PTUPB+CCl$_4$ group,

21   the level of HSC activation was not statistically different than the CCl$_4$ only group (p-value $<$

22   0.05), unlike the Celecoxib+CCl$_4$ group.

23   **Celecoxib lowered the tissue level of COX metabolites of arachidonic acid in CCl$_4$ treated**

14

MOL #111831

1   **mice**

2   We next examined the hepatic oxylipids by LC-MS/MS after solid phase extraction of

3   lipids from tissue lysates. A simplified diagram of these pathways is given in Supplemental Data

4   Figure S1. Although the differences did not reach statistical significance for every analyte, CCl_4

5   treatment displayed the same trend across several COX metabolites, raising their concentration

6   relative to the Control group (Figure 5 and Supplemental Data Table S4). Three metabolites in the

7   COX branch of the arachidonic acid cascade were significantly altered in the Celecoxib+CCl_4

8   group relative to either the Control or the CCl_4 only group (Figures 5A-D). The PGE_2 and PGD_2

9   levels were significantly higher in the CCl_4 only group compared to the Celecoxib+CCl_4 group.

10   Although they did not reach the level of statistical significance, PGJ_2 and 15-deoxy-$\Delta^{12,14}$-PGJ_2

11   show similar trends, the Celecoxib+CCl_4 group being lower than the CCl_4 only group.

12   Interestingly, the LOX metabolite of arachidonic acid, Lipoxin A_4 (LXA_4) was significantly

13   elevated by celecoxib (Figure 5E). The complete oxylipid profile is summarized in Supplemental

14   Data Table S4.

15   Finally, we determined the effect of the treatments on hepatic EET levels (Supplemental

16   Data Figure S3 and Table S4). Although the differences in the levels of these analytes did not

17   achieve statistical significance between any of the groups, the means for 8,9-, 11,12-, and 14,15-

18   EET were elevated in CCl_4 only group relative to the Control group (Figures S3A-C). The

19   Celecoxib+CCl_4 group had lowered 11,12- and 14,15- levels relative to the Control group (Figures

20   S3B-C). In the Celecoxib+TPPU+CCl_4 and PTUPB+CCl_4 groups, the EET levels were increased

21   relative to the Celecoxib+CCl_4 group (Figures S3A-C).

22

23

15

1   **Discussion**

2   There is a current disagreement in the literature regarding the use of celecoxib as a

3   treatment for liver damage and fibrosis (Hui et al., 2004; Paik et al., 2009; Wen et al., 2014; Yu et

4   al., 2009). Relevant to this study, opposing results have been reported in CCl_4 models of liver

5   fibrosis. In a short-term model, celecoxib reduced liver inflammation and damage during the early

6   phase of CCl_4 toxicity (Washino et al., 2010). A similar short-term study found that celecoxib

7   reduced markers of lipid peroxidation, but had no effect on hepatic toxicity or necrosis (Ekor et

8   al., 2013). Chavez et al reported that celecoxib reduced fibrosis as judged by collagen deposition

9   and other biochemical markers (Chavez et al., 2010). However, Hui et al reported that treatment

10   with celecoxib increased hepatic fibrosis, gauged by collagen deposition and MMP production

11   (Hui et al., 2006). In their discussion of these CCl_4 studies, Chavez et al suggested that differences

12   in CCl_4 model parameters might explain the conflicting results, in particular, the dose and length

13   of time of toxicant exposure (Chavez et al., 2010).

14   In the current study we obtained results similar to those reported by Hui et al after treatment

15   with celecoxib in their CCl_4 rat model of liver fibrosis, as well as those obtained by Reilly et al

16   using COX-2 knockout mice in an APAP model of acute liver damage (Hui et al., 2006; Reilly et

17   al., 2001). Like Hui et al, we found that celecoxib treatment increased the amount of collagen

18   deposition by approximately 25% compared to the CCl_4 only group (Hui et al., 2006). We also

19   observed an increase in αSMA staining, a marker for activated HSCs, in the Celecoxib+CCl_4 group

20   compared to the CCl_4 only group, though our model produced an almost twofold increase

21   compared to their reported 40% increase (Hui et al., 2006). However, we did not see an increase

22   in MMP-2 or MMP-9 mRNA expression in the Celecoxib+CCl_4 group compared to the CCl_4 only

23   group, unlike Hui et al. It should be kept in mind that Hui et al treated with a much higher dose of

16

1   CCl_4, 3200 mg/kg delivered twice weekly compared to our 80 mg/kg delivered twice weekly. Our

2   study also parallels results using COX-2 transgenic mice in a liver damage model. When COX-2

3   deficient mice were given a single bolus of APAP in an acute liver damage model (Reilly et al.,

4   2001), the $COX^{-/-}$ and $COX^{-/+}$ animals displayed a greater degree of bridging perivenous

5   hepatocyte necrosis than wild type (Reilly et al., 2001). Similarly, we observed an increase in

6   hepatic necrosis in the Celecoxib+CCl_4 group compared to the CCl_4 only group. Although the

7   mechanism of toxicity of APAP and CCl_4 are different, this may indicate that celecoxib accelerates

8   hepatic necrosis in models that involve severe oxidative stress.

9   We used two pharmacological tools in addition to celecoxib to perturb the oxylipid

10   homeostasis, TPPU and PTUPB. TPPU is a potent inhibitor of soluble epoxide hydrolase, an

11   enzyme that metabolizes epoxy fatty acids (Rose et al., 2010). In previous studies we have reported

12   that TPPU treatment reduces hepatic fibrosis (Harris et al., 2015; Harris et al., 2016). PTUPB

13   contains the pharmacophores from both celecoxib and TPPU and inhibits both enzymes (Hwang

14   et al., 2011). We found that treatment with PTUPB or co-treatment with TPPU and celecoxib

15   decreased the elevated collagen deposition observed in the Celecoxib+CCl_4 group. The most

16   striking result obtained with these inhibitors concerns the elevated αSMA in the Celecoxib+CCl_4

17   group. While not returning αSMA levels to that of the Control group, co-treatment with the sEH

18   inhibitor attenuated the elevated αSMA expression observed in the Celecoxib+CCl_4 group.

19   Changes in associated oxylipid mediators will be discussed below. Interestingly, we saw a slight

20   reduction in F4/80 expression, a marker of macrophages, in the Celecoxib+CCl_4 group compared

21   to the CCl_4 only group, indicating that the increase in fibrosis in the Celecoxib+CCl_4 group is not

22   due to increased macrophage migration.

23   The downstream COX-2 metabolites PGE_2 and 15-deoxy-$\Delta^{12,14}$-PGJ_2 have been proposed

17

1 to mediate both the pro- and anti-fibrotic effects of COX-2 inhibition or gene deletion, depending

2 on the model. In general, prostaglandins have been shown to have organ protective effects in the

3 liver (Reilly et al., 2001), and PGE_2 reduced collagen production in a human cell culture model of

4 HSCs (Hui et al., 2004). Results that support a pro-fibrotic role for COX-2 downstream metabolites

5 include the observation that plasma PGE_2 levels were elevated after treatment with TAA (Wen et

6 al., 2014). In a separate study using the BDL and TAA models, PGE_2 levels were increased in the

7 fibrotic animals and reduced after treatment with celecoxib, with an accompanying attenuation of

8 fibrosis (Paik et al., 2009). 15-deoxy-$\Delta^{12,14}$-PGJ_2 is another potential pro-fibrotic downstream

9 COX-2 metabolite elevated in the serum of fibrotic rats treated with CCl_4 (Planaguma et al., 2005).

10 However, 15-deoxy-$\Delta^{12,14}$-PGJ_2 has also been shown to induce apoptosis of human

11 myofibroblasts, a process that contributes to the resolution of fibrosis (Li et al., 2001).

12 We performed an analysis of oxylipids of the arachidonic acid cascade to determine the

13 effect of COX-2 and sEH inhibition. Overall, we found that COX metabolites were elevated in the

14 CCl_4 only group, though the levels did not reach statistical significance in most cases. PGE_2 levels

15 were elevated in the CCl_4 only group and substantially lowered in the Celecoxib+CCl_4 group as

16 expected for a COX inhibitor. As outlined above, there was extensive fibrosis in both of these

17 groups, the greatest degree of fibrosis found in the Celecoxib+CCl_4 group where the lowest PGE_2

18 level was detected. Consistent with an anti-inflammatory effect of celecoxib in the liver, LXA_4

19 was greatly elevated by celecoxib. Interestingly, treatment with TPPU and celecoxib or the dual

20 COX-2/sEH inhibitor in the CCl_4 background raised PGE_2 levels and lowed LXA_4 levels compared

21 to the Celecoxib+CCl_4 group, in both cases bringing the levels of these lipid mediators closer to

22 those observed in the Control group. It is possible that a drastic reduction in inflammatory

23 processes in the CCl_4 background results in even greater damage to the liver and that, depending

18

1   on the inflammatory state of the liver, an elevation in PGE_2 levels will either increase or decrease

2   liver damage and fibrosis. This might explain some of the contradicting conclusions regarding the

3   role of PGE_2 in different liver fibrosis models.

4   There was high variation in the PGJ_2 and 15-deoxy-$\Delta^{12,14}$-PGJ_2 levels, but the trend of

5   metabolites was similar. While CCl_4 elevated their mean levels compared to the Control group,

6   the levels were slightly decreased in other groups. Based on these data, the 15-deoxy-$\Delta^{12,14}$-PGJ_2

7   levels do not explain the increased fibrosis in the Celeoxib+CCl_4 group, or the attenuation in

8   fibrosis after TPPU co-treatment.

9   sEH inhibitors and presumably the underlying elevation in epoxy fatty acid chemical

10   mediators have been shown to reduce pathological fibrosis in several models (Hye Khan et al.,

11   2016; Kim et al., 2014; Liao et al., 2016; Zhou et al., 2016) including ischemia driven heart failure

12   (Sirish et al., 2013). Earlier we demonstrated that sEHI reduced hepatic fibrosis in the same CCl_4

13   model used in this study (Harris et al., 2015; Harris et al., 2016). However, unlike some other

14   pathological changes reversed by sEHI, the effects were not enhanced by a diet depleted in ω-6

15   relative to ω-3 fatty acids.

16   sEH inhibitors synergize with NSAIDs in many biological systems (Hwang et al., 2011;

17   Hye Khan et al., 2016; Schmelzer et al., 2006; Zhang et al., 2014). Surprisingly, sEH inhibitors

18   prevent and reverse gastrointestinal erosion caused by the NSAID diclofenac (Goswami et al.,

19   2017; Goswami et al., 2016), and indomethacin (Goswami, forthcoming), and in mice they block

20   some of the cardiovascular effects caused by COX-2 inhibitors possibly by returning the enhanced

21   blood levels of TXA_2 to PGI_2 to more normal levels (Schmelzer et al., 2006). Since celecoxib is a

22   selective COX-2 inhibitor and PTUPB is a highly selective COX-2 inhibitor, we expected a strong

23   positive synergistic effect between the sEHI TPPU and celecoxib and an dramatic reduction in

19

1   fibrosis with PTUPB. Surprisingly, the profibrotic effect of celecoxib in our CCl_4 model

2   overpowered possible positive synergistic interaction with sEHI giving only moderate efficacy in

3   reducing fibrosis and fibrosis markers. This result suggests that celecoxib in not an attractive drug

4   to treat hepatic in a system driven my pathological peroxidation. However, both sEHI alone and

5   dual COX/sEH inhibitors may be worth examining in hepatic fibrosis models driven by agents

6   other than CCl_4. In patients with hepatic fibrosis who are on celecoxib or other NSAIDs for a

7   difference disease, sEHI may ameliorate the exacerbation of the hepatic fibrosis by celecoxib.

8   Finally, although the differences observed in the EETs did not achieve statistical

9   significance, the trends suggest that the sEH inhibitors were able to elevate hepatic EET levels,

10   although CCl_4 treatment also raised the level of these oxylipids. Given the variation in the data one

11   must use caution in interpretation, but it is possible that the slight increase in EET levels after CCl_4

12   treatment is insufficient to counteract pro-fibrotic environment and that the further increase in

13   EETs caused by sEH inhibition tips the balance, partially countering the pro-fibrotic effects of

14   celecoxib in the CCl_4 background. In the oxylipin, as well as the mRNA expression and

15   histological analyses, small n sizes might be responsible for trends not reaching significance in

16   this study. Given the variability of fibrotic and inflammatory responses in chronic studies, small

17   group sizes can limit the ability to detect differences between groups.

18   Due to the differences in animal models and the dose of celecoxib used, the effectiveness

19   of COX-2 inhibition as a treatment of liver fibrosis is questionable. In the current study, we have

20   an indication that oxidized fatty acids other than COX-2 metabolites of arachidonic acid may be

21   involved in the pro-fibrotic properties of celecoxib in a CCl_4 mouse model of liver fibrosis. Given

22   their effectiveness in modulating the EETs as well as their anti-fibrotic effects in the liver and

23   other tissues, sEHI are promising tools for the study of the role of these oxylipids in hepatic fibrosis

MOL #111831

1   and damage.

2

3

4

5

6

7

8

9

10

11

12

13

14

15

16

17

18

19

20

21

22

23

21

MOL #111831

1 **Author Contributions**

2 *Participated in research design:* Harris, Kodani, Hammock.

3 *Conducted experiments:* Harris and Rand.

4 *Contributed new reagents or analytic tools:* Rand, Yang, and Hwang.

5 *Performed data analysis:* Harris, Imai.

6 *Wrote or contributed to the writing of the manuscript:* Harris, Imai and Hammock.

7

8

9

10

11

12

13

14

15

16

17

18

19

20

21

22

23

MOL #111831

1   **References**

2   Bessone F, Hernandez N, Roma MG, Ridruejo E, Mendizabal M, Medina-Caliz I, Robles-Diaz M,

3   Lucena MI and Andrade RJ (2016) Hepatotoxicity induced by coxibs: how concerned

4   should we be? *Expert Opin Drug Saf* **15**(11): 1463-1475.

5   Chavez E, Segovia J, Shibayama M, Tsutsumi V, Vergara P, Castro-Sanchez L, Salazar EP,

6   Moreno MG and Muriel P (2010) Antifibrotic and fibrolytic properties of celecoxib in liver

7   damage induced by carbon tetrachloride in the rat. *Liver Int* **30**(7): 969-978.

8   Constandinou C, Henderson N and Iredale JP (2005) Modeling liver fibrosis in rodents. *Methods*

9   *Mol Med* **117**: 237-250.

10 Ekor M, Odewabi AO, Kale OE, Adesanoye OA and Bamidele TO (2013) Celecoxib, a selective

11   cyclooxygenase-2 inhibitor, lowers plasma cholesterol and attenuates hepatic lipid

12   peroxidation during carbon-tetrachloride-associated hepatotoxicity in rats. *Drug Chem*

13   *Toxicol* **36**(1): 1-8.

14 Goswami SK, Rand AA, Wan D, Yang J, Inceoglu B, Thomas M, Morisseau C, Yang GY and

15   Hammock BD (2017) Pharmacological inhibition of soluble epoxide hydrolase or genetic

16   deletion reduces diclofenac-induced gastric ulcers. *Life Sci* **180**: 114-122.

17 Goswami SK, Wan D, Yang J, Trindade da Silva CA, Morisseau C, Kodani SD, Yang GY,

18   Inceoglu B and Hammock BD (2016) Anti-ulcer efficacy of soluble epoxide hydrolase

19   inhibitor TPPU on diclofenac-induced intestinal ulcers. *J Pharmacol Exp Ther* **357**(3):

20   529-536.

21 Harris TR, Bettaieb A, Kodani S, Dong H, Myers R, Chiamvimonvat N, Haj FG and Hammock

22   BD (2015) Inhibition of soluble epoxide hydrolase attenuates hepatic fibrosis and

23

1   endoplasmic reticulum stress induced by carbon tetrachloride in mice. *Toxicol Appl*

2   *Pharmacol* **286**(2): 102-111.

3   Harris TR, Kodani S, Yang J, Imai DM and Hammock BD (2016) An omega-3-enriched diet alone

4   does not attenuate CCl4-induced hepatic fibrosis. *J Nutr Biochem* **38**: 93-101.

5   Hui AY, Dannenberg AJ, Sung JJ, Subbaramaiah K, Du B, Olinga P and Friedman SL (2004)

6   Prostaglandin E2 inhibits transforming growth factor beta 1-mediated induction of collagen

7   alpha 1(I) in hepatic stellate cells. *J Hepatol* **41**(2): 251-258.

8   Hui AY, Leung WK, Chan HL, Chan FK, Go MY, Chan KK, Tang BD, Chu ES and Sung JJ

9   (2006) Effect of celecoxib on experimental liver fibrosis in rat. *Liver Int* **26**(1): 125-136.

10   Hwang SH, Wagner KM, Morisseau C, Liu JY, Dong H, Wecksler AT and Hammock BD (2011)

11   Synthesis and structure-activity relationship studies of urea-containing pyrazoles as dual

12   inhibitors of cyclooxygenase-2 and soluble epoxide hydrolase. *J Med Chem* **54**(8): 3037-

13   3050.

14   Hye Khan MA, Hwang SH, Sharma A, Corbett JA, Hammock BD and Imig JD (2016) A dual

15   COX-2/sEH inhibitor improves the metabolic profile and reduces kidney injury in Zucker

16   diabetic fatty rat. *Prostaglandins Other Lipid Mediat* **125**: 40-47.

17   Kim J, Imig JD, Yang J, Hammock BD and Padanilam BJ (2014) Inhibition of soluble epoxide

18   hydrolase prevents renal interstitial fibrosis and inflammation. *Am J Physiol Renal Physiol*

19   **307**(8): F971-980.

20   Li L, Tao J, Davaille J, Feral C, Mallat A, Rieusset J, Vidal H and Lotersztajn S (2001) 15-deoxy-

21   Delta 12,14-prostaglandin J2 induces apoptosis of human hepatic myofibroblasts. A

22   pathway involving oxidative stress independently of peroxisome-proliferator-activated

23   receptors. *J Biol Chem* **276**(41): 38152-38158.

1   Liao J, Hwang SH, Li H, Liu JY, Hammock BD and Yang GY (2016) Inhibition of chronic
2   pancreatitis and murine pancreatic intraepithelial neoplasia by a dual inhibitor of c-RAF
3   and soluble epoxide hydrolase in LSL-KrasG(1)(2)D/Pdx-1-Cre mice. *Anticancer Res*
4   **36**(1): 27-37.

5   Liedtke C, Luedde T, Sauerbruch T, Scholten D, Streetz K, Tacke F, Tolba R, Trautwein C,
6   Trebicka J and Weiskirchen R (2013) Experimental liver fibrosis research: update on
7   animal models, legal issues and translational aspects. *Fibrogenesis Tissue Repair* **6**(1): 19.

8   Martinez AK, Maroni L, Marzioni M, Ahmed ST, Milad M, Ray D, Alpini G and Glaser SS (2014)
9   Mouse models of liver fibrosis mimic human liver fibrosis of different etiologies. *Curr*
10   *Pathobiol Rep* **2**(4): 143-153.

11   Morisseau C and Hammock BD (2013) Impact of soluble epoxide hydrolase and epoxyeicosanoids
12   on human health. *Annu Rev Pharmacol Toxicol* **53**: 37-58.

13   Paik YH, Kim JK, Lee JI, Kang SH, Kim DY, An SH, Lee SJ, Lee DK, Han KH, Chon CY, Lee
14   SI, Lee KS and Brenner DA (2009) Celecoxib induces hepatic stellate cell apoptosis
15   through inhibition of Akt activation and suppresses hepatic fibrosis in rats. *Gut* **58**(11):
16   1517-1527.

17   Pellicoro A, Ramachandran P, Iredale JP and Fallowfield JA (2014) Liver fibrosis and repair:
18   immune regulation of wound healing in a solid organ. *Nat Rev Immunol* **14**(3): 181-194.

19   Planaguma A, Claria J, Miquel R, Lopez-Parra M, Titos E, Masferrer JL, Arroyo V and Rodes J
20   (2005) The selective cyclooxygenase-2 inhibitor SC-236 reduces liver fibrosis by
21   mechanisms involving non-parenchymal cell apoptosis and PPARgamma activation.
22   *FASEB J* **19**(9): 1120-1122.

1   Reddy GK and Enwemeka CS (1996) A simplified method for the analysis of hydroxyproline in

2   biological tissues. *Clin Biochem* **29**(3): 225-229.

3   Reilly TP, Brady JN, Marchick MR, Bourdi M, George JW, Radonovich MF, Pise-Masison CA

4   and Pohl LR (2001) A protective role for cyclooxygenase-2 in drug-induced liver injury in

5   mice. *Chem Res Toxicol* **14**(12): 1620-1628.

6   Rose TE, Morisseau C, Liu JY, Inceoglu B, Jones PD, Sanborn JR and Hammock BD (2010) 1-

7   Aryl-3-(1-acylpiperidin-4-yl)urea inhibitors of human and murine soluble epoxide

8   hydrolase: structure-activity relationships, pharmacokinetics, and reduction of

9   inflammatory pain. *J Med Chem* **53**(19): 7067-7075.

10 Sacerdoti D, Pesce P, Di Pascoli M, Brocco S, Cecchetto L and Bolognesi M (2015) Arachidonic

11   acid metabolites and endothelial dysfunction of portal hypertension. *Prostaglandins Other

12   Lipid Mediat* **120**: 80-90.

13 Schmelzer KR, Inceoglu B, Kubala L, Kim IH, Jinks SL, Eiserich JP and Hammock BD (2006)

14   Enhancement of antinociception by coadministration of nonsteroidal anti-inflammatory

15   drugs and soluble epoxide hydrolase inhibitors. *Proc Natl Acad Sci U S A* **103**(37): 13646-

16   13651.

17 Shi S and Klotz U (2008) Clinical use and pharmacological properties of selective COX-2

18   inhibitors. *Eur J Clin Pharmacol* **64**(3): 233-252.

19 Sirish P, Li N, Liu JY, Lee KS, Hwang SH, Qiu H, Zhao C, Ma SM, Lopez JE, Hammock BD and

20   Chiamvimonvat N (2013) Unique mechanistic insights into the beneficial effects of soluble

21   epoxide hydrolase inhibitors in the prevention of cardiac fibrosis. *Proc Natl Acad Sci U S

22   A* **110**(14): 5618-5623.

1   Washino Y, Koga E, Kitamura Y, Kamikawa C, Kobayashi K, Nakagawa T, Nakazaki C, Ichi I

2   and Kojo S (2010) Effect of celecoxib, a selective cyclooxygenase-2 inhibitor on carbon

3   tetrachloride intoxication in rats. *Biol Pharm Bull* **33**(4): 707-709.

4   Wen SL, Gao JH, Yang WJ, Lu YY, Tong H, Huang ZY, Liu ZX and Tang CW (2014) Celecoxib

5   attenuates hepatic cirrhosis through inhibition of epithelial-to-mesenchymal transition of

6   hepatocytes. *J Gastroenterol Hepatol* **29**(11): 1932-1942.

7   Yu J, Hui AY, Chu ES, Go MY, Cheung KF, Wu CW, Chan HL and Sung JJ (2009) The anti-

8   inflammatory effect of celecoxib does not prevent liver fibrosis in bile duct-ligated rats.

9   *Liver Int* **29**(1): 25-36.

10 Zhang G, Panigrahy D, Hwang SH, Yang J, Mahakian LM, Wettersten HI, Liu JY, Wang Y,

11   Ingham ES, Tam S, Kieran MW, Weiss RH, Ferrara KW and Hammock BD (2014) Dual

12   inhibition of cyclooxygenase-2 and soluble epoxide hydrolase synergistically suppresses

13   primary tumor growth and metastasis. *Proc Natl Acad Sci U S A* **111**(30): 11127-11132.

14 Zhou Y, Yang J, Sun GY, Liu T, Duan JX, Zhou HF, Lee KS, Hammock BD, Fang X, Jiang JX

15   and Guan CX (2016) Soluble epoxide hydrolase inhibitor 1-trifluoromethoxyphenyl-3- (1-

16   propionylpiperidin-4-yl) urea attenuates bleomycin-induced pulmonary fibrosis in mice.

17   *Cell Tissue Res* **363**(2): 399-409.

18

19

20

21

22

23

MOL #111831

10

11

12

13

14

15

16

17

18

19

20

21

22

23

1   **Legends for Figures**

2   Figure 1. Celecoxib increases the collagen deposition caused by CCl_4 treatment. Mice were

3   injected (i.p.) with CCl_4 for 5 weeks. The inhibitors were administered subcutaneously via osmotic

4   minipumps that delivered the compounds at a calculated dose of 10 mg/kg/day for a 30 gram

5   mouse. A-E) Representative slides of liver sections stained with trichrome (40x). F) Quantification

6   of staining as determined by the Aperio positive pixel count algorithm. The negative pixel ratio

7   represents the % area of collagen deposition, which is stained blue by the Trichrome stain. G)

8   Quantification of hepatic levels of hydroxyproline. Error bars represent standard deviation. *p-

9   value vs. Control group < 0.05. $^{\ddagger}p$-value vs. CCl_4 only group < 0.05. #p-value vs. Celecoxib+CCl_4

10   group < 0.05. N = 6 for Celecoxib+CCl_4 group, N = 5 for all other groups. Statistical tests are

11   described in Materials and Methods. The raw data used for this figure is reported in Supplemental

12   Data Table S3.

13

14   Figure 2. Celecoxib modulates markers of hepatic fibrosis that are increased after CCl_4 treatment.

15   Total RNA from hepatic tissue and cDNA were prepared as described. Quantitative PCR was

16   performed using Taqman probes on an Applied Biosystems Fast PCR instrument as described.

17   Mice were injected (i.p.) with CCl_4 for 5 weeks. The inhibitors were administered subcutaneously

18   via osmotic minipumps that delivered the compounds at a calculated dose of 10 mg/kg/day for a

19   30 gram mouse. Error bars represent standard deviation. *p-value vs. Control group < 0.05. N = 3

20   for Celecoxib+CCl_4 group, N = 4 for all other groups. Statistical tests are described in Materials

21   and Methods. The raw data used for this figure is reported in Supplemental Data Table S3.

22

1   Figure 3. Celecoxib attenuates the increased recruitment of macrophages caused by CCl_4

2   treatment. (A-E) IHC on liver tissue with an anti-F4/80 antibody (40x). (F) Quantification of IHC

3   stain using the Aperio positive pixel count algorithm. Mice were injected (i.p.) with CCl_4 for 5

4   weeks. The inhibitors were administered subcutaneously via osmotic minipumps that delivered the

5   compounds at a calculated dose of 10 mg/kg/day for a 30 gram mouse. Error bars represent

6   standard deviation. *p-value vs. Control group < 0.05. N = 5. Statistical tests are described in

7   Materials and Methods. The raw data used for this figure is reported in Supplemental Data Table

8   S3.

9

10   Figure 4. Celecoxib further increases the hepatic stellate cell activation triggered by CCl_4

11   treatment. (A-E) IHC on liver tissue with an anti-αSMA antibody (40x). (F) Quantification of stain

12   using the Aperio positive pixel count algorithm. Mice were injected (i.p.) with CCl_4 for 5 weeks.

13   The inhibitors were administered subcutaneously via osmotic minipumps that delivered the

14   compounds at a calculated dose of 10 mg/kg/day for a 30 gram mouse. Error bars represent

15   standard deviation. *p-value vs. Control group < 0.05. ‡p-value vs. CCl_4 only group < 0.05. #p-

16   value vs. Celecoxib+CCl_4 group < 0.05. N = 5. Statistical tests are described in Materials and

17   Methods. The raw data used for this figure is reported in Supplemental Data Table S3.

18

19   Figure 5. Celecoxib modulates the increase in metabolites in the COX and LOX branches of the

20   arachidonic acid cascade caused by CCl_4 treatment. (A-D) Hepatic tissue levels of metabolites in

21   the COX branch. (E) Hepatic tissue levels of Lipoxin A_4, a metabolite in the LOX branch. Tissue

22   levels of compounds were analyzed by LC-MS/MS after solid phase extraction as described in

23   Materials and Methods. Mice were injected (i.p.) with CCl_4 for 5 weeks. The inhibitors were

MOL #111831

1 administered subcutaneously via osmotic minipumps that delivered the compounds at a calculated

2 dose of 10 mg/kg/day for a 30 gram mouse. For a simplified diagram of these pathways see

3 Supplemental Data Figure S1. Error bars represent standard deviation. *p-value vs. Control group

4 < 0.05. ‡p-value vs. CCl$_4$ only group < 0.05. #p-value vs. Celecoxib+CCl$_4$ group < 0.05. N = 6 for

5 Celecoxib+CCl$_4$ group, N = 5 for all other groups. Statistical tests are described in Materials and

6 Methods. The raw data used for this figure is reported in Supplemental Data Table S3.

7

8

9

10

11

12

13

14

15

16

17

18

19

20

21

22

23

MOL #111831

1   **Tables**

2   Table 1. Histological scoring of H&E-stained sections for inflammation, fibrosis and cellular

3   damage on a 0-3 scale as described in Supplemental Data Table S1.

Experimental Group	Vacuolation	Necrosis	Lipofuscinosi	Fibrosis	Inflammatio	Proliferation	Cumulative
Control	0	0	0	0	0	0	0
Control	0	0	0	0	0	0	0
Control	0	0	0	0	0	0	0
Control	0	0	0	0	0	0	0
Control	0	0	0	0	0	0	0
CCl_4 only	2	0	1	1	1	1	6
CCl_4 only	1	0	1	1	1	0	4
CCl_4 only	1	0	1	1	1	1	5
CCl_4 only	0	0	1	1	1	1	4
CCl_4 only	1	1	1	1	1	2	7
Celecoxib+CCl_4	3	2	1	2	1	2	11
Celecoxib+CCl_4	3	2	1	2	1	2	11
Celecoxib+CCl_4	3	2	1	1	1	2	10
Celecoxib+CCl_4	3	3	1	1	1	2	11
Celecoxib+CCl_4	3	2	1	2	1	3	12
Celecoxib+CCl_4	3	2	1	2	1	2	11
Celecoxib+TPPU+CCl_4	3	0	1	2	1	1	8

MOL #111831

1								
	Celecoxib+TPPU+CCl$_4$	3	0	1	1	1	1	7
	Celecoxib+TPPU+CCl$_4$	3	0	1	2	1	1	8
	Celecoxib+TPPU+CCl$_4$	3	0	1	1	1	1	7
	Celecoxib+TPPU+CCl$_4$	3	2	1	1	1	3	11
	PTUPB+CCl$_4$	3	1	1	1	1	1	8
	PTUPB+CCl$_4$	2	2	1	1	1	1	8
	PTUPB+CCl$_4$	1	0	1	2	1	2	7
	PTUPB+CCl$_4$	3	2	1	2	1	2	11
	PTUPB+CCl$_4$	3	1	1	2	1	1	9
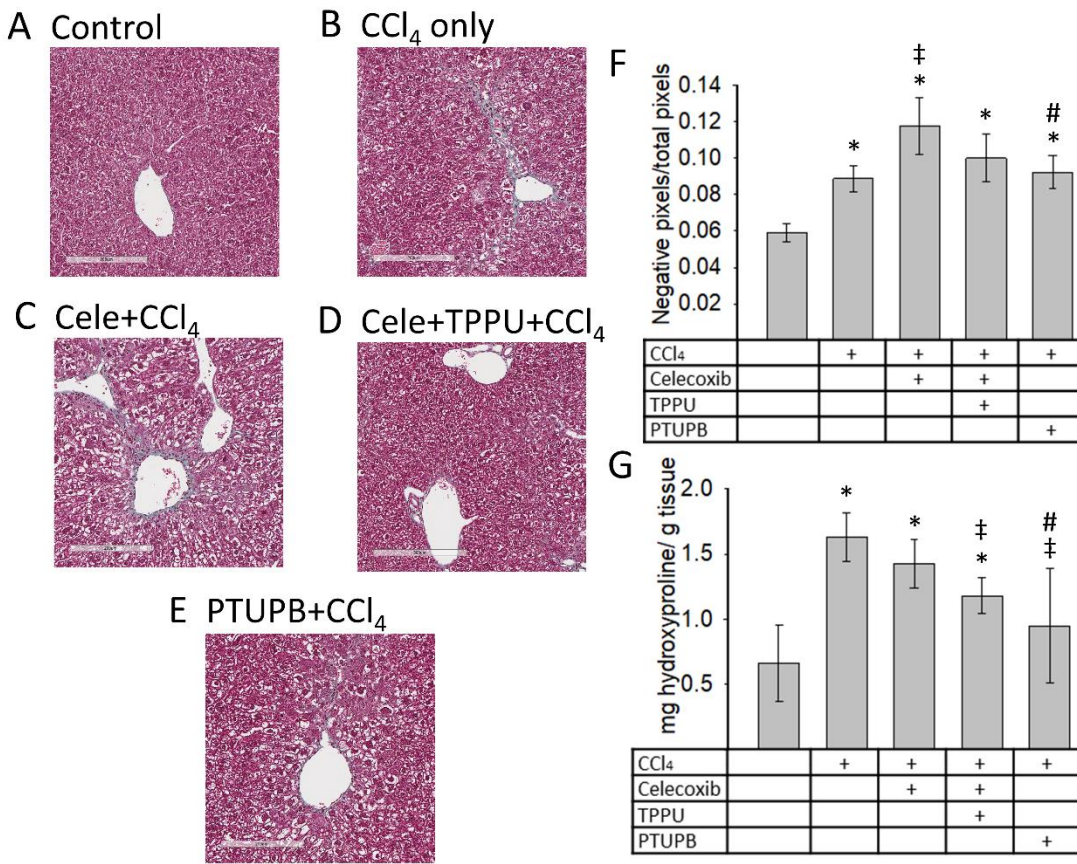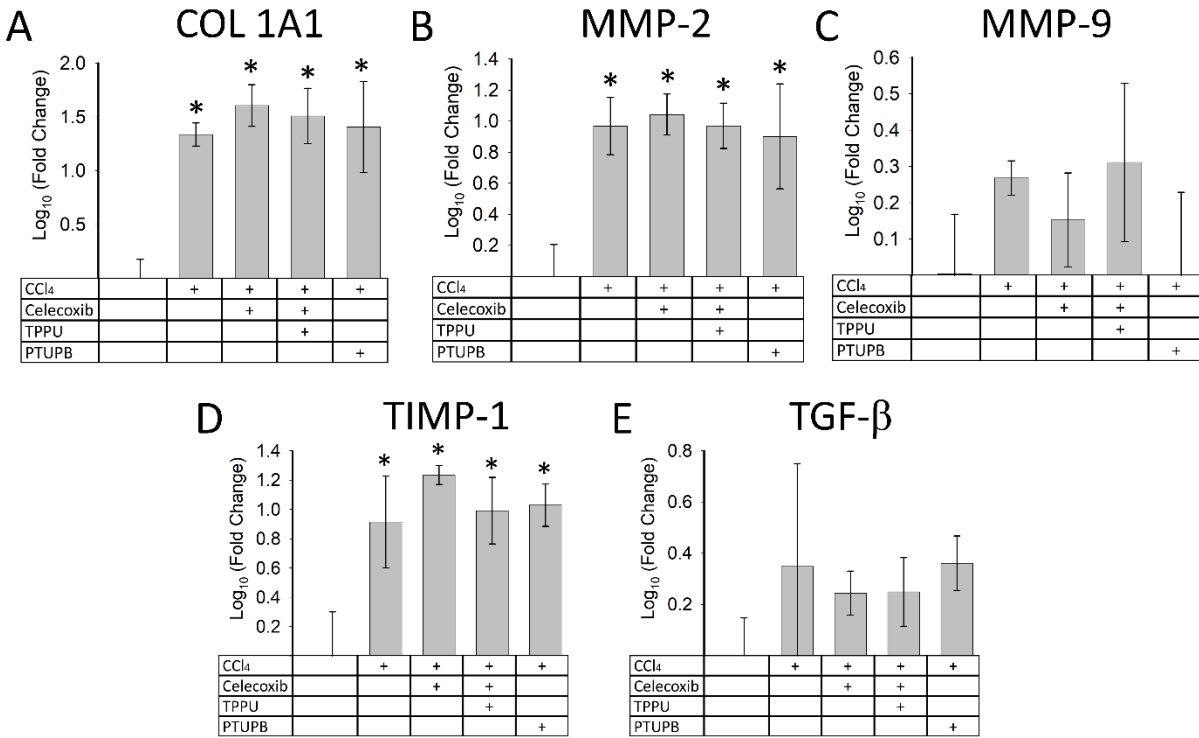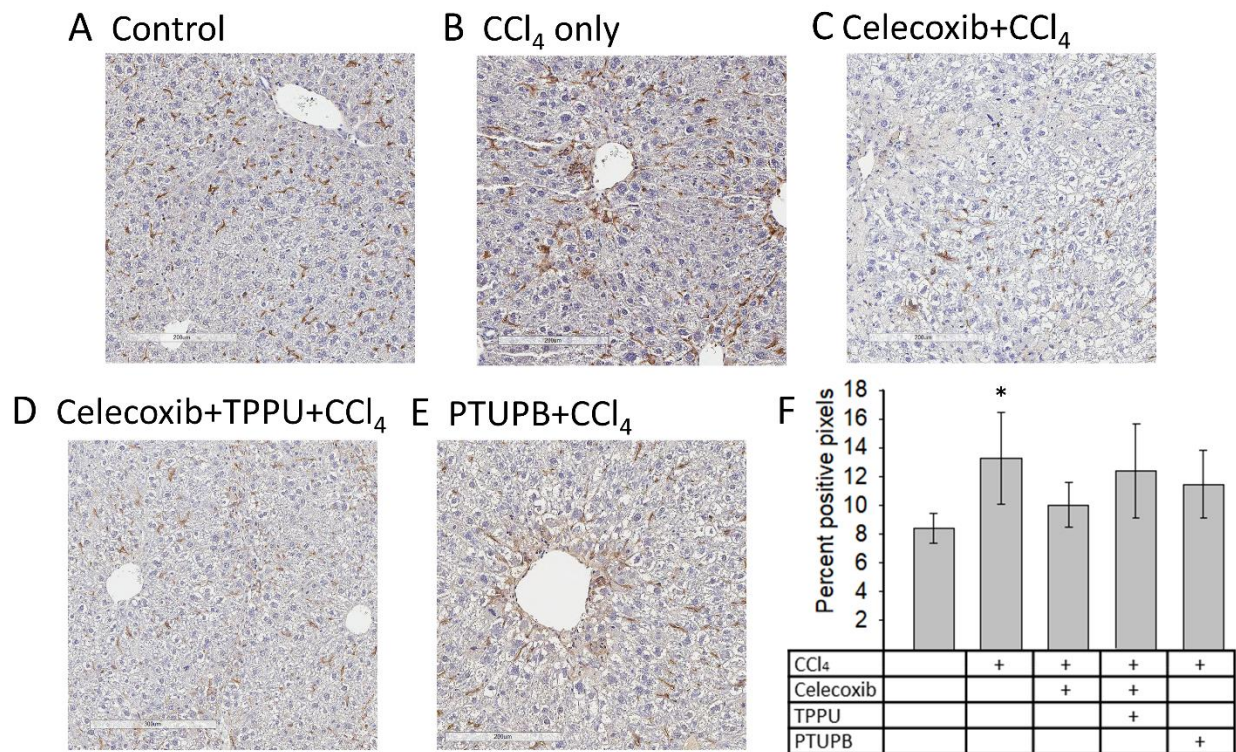
Figure 1
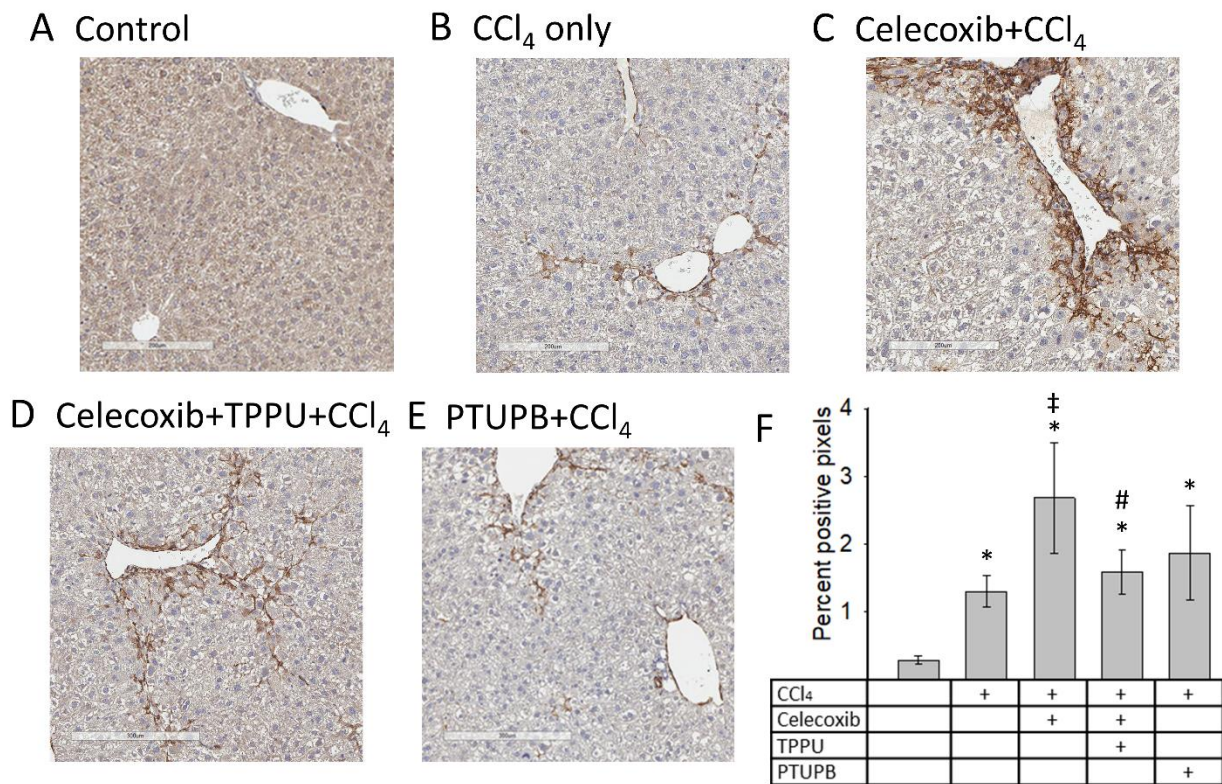
Figure 2

Figure 3

Figure 4

MOL #111831

Figure 5